Thermal Analysis of Cables in Unfilled Troughs: Investigation of the IEC Standard and a Methodical Approach for Cable Rating

Matthew Terracciano, Sujit Purushothaman, *Student Member, IEEE*, Francisco de León, *Senior Member, IEEE*, and Alireza Vashghani Farahani, *Member, IEEE*

Abstract—A robust algorithm, based on relaxation, is proposed for the implementation of the IEC Standard method for rating cables installed in unfilled troughs. Through hundreds of finite-element simulations, the validity range of the standardized equations is established. Studies are performed by varying the following parameters over a wide range: trough size, ambient air temperature, trough aspect ratio, position of cables, cable operating temperature, and intensity of solar radiation. A physically consistent analog thermal-electric equivalent circuit is proposed for the thermal rating of cables installed in unfilled troughs. In contrast with the standards, the equivalent circuit offers a methodological approach that considers all heat-transfer phenomena involved in cables in troughs, for example, the conduction of heat through the cable layers, the heat convection and radiation inside the trough, the conduction in the trough itself and soil, the convection to the surface air, and the solar radiation. Extensive finite-element verification in steady state and transients demonstrates the accuracy of the proposed equivalent circuit.

Index Terms—Ampacity, cable thermal rating, finite elements, intensity of solar radiation, unfilled troughs.

I. INTRODUCTION

CABLE THERMAL analysis is an important aspect of the design of electrical power systems. The maximum current that a cable can carry depends on how efficiently the inherent cable losses can be dissipated.

Cables are installed in varied arrangements; for example: directly buried, in duct banks, in backfills, in filled or unfilled troughs, in tunnels, in casings, etc. Anders [1] has compiled the knowledge available today on cable thermal rating. The most commonly used methods for rating cables are the Neher–McGrath method [2] (adopted by the IEEE [3]) and the IEC Standards method [4]–[8].

The IEC Standard IEC-60287-2-1 [6] in Section 2.2.6.2 gives an empirical formula to rate cables in unfilled troughs that have the top flush with the air/soil interface. The temperature rise of the air inside the trough above (external) air ambient is given by

$$\Delta T = \frac{W_{\text{TOT}}}{3p} \qquad (1)$$

where W_{TOT} is the total power dissipated in the trough per unit length (in watts per meter) and p (in meters) is that part of the trough perimeter which is effective for heat dissipation. In the studies of this paper, we have assumed that the trough is flushed with the surface and the cover is exposed to the sun. Therefore, the cover is not included in the value of p. Under these conditions, the rating of a cable in the trough is to be calculated as for a cable in free air, but the ambient temperature increased by ΔT. The standard also issues the following warning: "NOTE The validity of this formula is at present under investigation."

The formula is very simple and takes into account only total loss and trough size through its perimeter. It does not consider any of the following parameters that may impact the thermal behavior: trough aspect ratio, position of cables, ambient air (external), soil and trough thermal conductivities, cable surface emissivity, and intensity of solar radiation.

Slaninka used conformal mapping in 1965 to obtain an analytical expression for the contribution to the external thermal resistance made by the trough and the surrounding soil [9]. It was assumed that the trough and the ground surface are isotherms. A recent paper by Anders, Coates, and Chaaban [10] reviews and compares different existing and proposed methods to rate installations inside an unfilled trough. Based on the measurements carried out by the ERA Technology, a new approach to calculate the temperature rise inside the trough is proposed. This paper investigates the effect of many different parameters, such as the thermal resistivity of soil and trough as well as the solar radiation and wind velocity which affect the maximum temperature reached within an unfilled trough.

The contributions of this paper are as follows: 1) to propose a robust computer algorithm to rate cables in unfilled troughs per IEC Standards; it is known that simple fixed-point (Gauss-Seidel type of) iterations frequently yield divergent results; 2) to find the validity range of the IEC method through finite-element simulations; this includes: the size (perimeter) of the trough, the aspect ratio of the trough, the position of the cables in the trough; and 3) to propose a methodological approach, derived

from basic principles, to study the thermal behavior of cables installed in unfilled troughs. The method includes in the calculation the effects of the trough, the soil, the emissivity of the cable surface, and the intensity of solar radiation. The proposed model is compatible with the IEC standardized methods used to rate underground cables since it is an analog thermal-electrical circuit.

This paper is organized as follows: Section II presents a method to overcome technical difficulties in the iterative methods used for implementing the IEC standard. In Section III, the parameters of trough perimeter, aspect ratio, and position of cables are varied to verify the validity of the IEC standard. The effects of solar intensity, long-duration transients, and surface emmissivity are also studied. Sections IV and V present the equivalent thermal circuit and the evaluation of the nonlinear thermal resistance of air around the cable.

II. PRACTICAL IMPLEMENTATION OF THE IEC STANDARD METHOD

The rating of a cable installation inside unfilled troughs, based on the IEC standard, is done as the rating of a corresponding installation in free air. The equivalent installation in free air is composed of the same configuration of cables inside the trough but the ambient temperature is increased by ΔT given in (1).

The losses inside the trough depend on the current which, in turn, depends on the inside temperature. On the other hand, the inside temperature itself is determined by the total loss (1). This mutual dependence between the total loss and the temperature inside the trough suggests the use of an iterative approach. In the final (or converged) solution, the total losses inside the trough and the temperature rise inside the trough above the ambient should satisfy (1).

An intuitive iterative approach starts with an initial guess for the temperature inside the trough T_0. This can be the air ambient temperature above ground T_a. Starting with this initial guess for the temperature inside the trough, the IEC standard method to rate the corresponding installation in free air can be applied. In general, the total loss W_0 obtained for the corresponding installation in free air will not satisfy (1). However, (1) can be used to compute a "better" second guess using

$$T_{i+1} = T_a + \frac{W_i}{3p}. \qquad (2)$$

With this new temperature inside the trough, the main iteration loop explained before is repeated. The air ambient is set to T_1 and the current I_1 and the total loss W_1 are obtained. One can check whether the new total loss W_1 and the temperature inside the trough $T_2 = \Delta T_1 + T_a$ satisfy (1). It turns out that this is almost never the case. In fact, the sequence of solutions T_i, W_i, and I_i for any typical installation will not converge to the set of final solutions for the inside temperature of the trough.

Extensive experimentation with different cable installations and initial guesses has shown that the fixed-point iteration described before rarely arrives at the correct results. The iteration frequently diverges or toggles between a high and low value. The use of (de-) acceleration factors in the Gauss–Seidel method
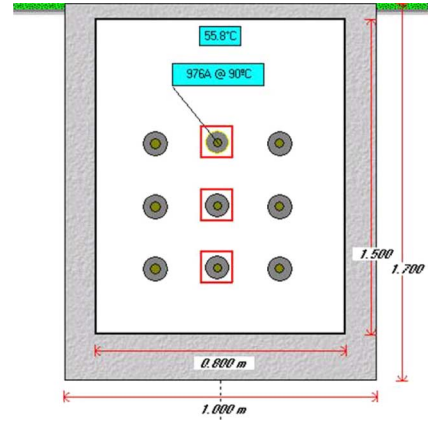
Fig. 1. Example of unfilled trough installation with lid flush with the surface.

also proved to be ineffective. Although convergence is achievable with large de-acceleration factors for many examples, the convergence is slow and still not guaranteed.

Successive relaxation is proposed in this paper to obtain consistently accurate solutions for the thermal rating of cables inside unfilled troughs [15]. The method is based on (1), but the new value for the temperature inside the trough is computed as a linear combination of the previous value and the one computed with (1) as follows:

$$T_{i+1} = (1 - \lambda)T_i + \lambda\left(T_a + \frac{W_i}{3p}\right) \qquad (3)$$

where λ is the relaxation parameter that is normally between 0 and 1. When $\lambda = 1$, (3) reduces to (2). Here, $\lambda = 0.5$ is used. With this approach, the sequence of current ratings I_i, total loss W_i, and the temperature inside the unfilled trough T_i converge within a few iterations to the solutions that satisfy (1).

Fig. 1 shows an example of an unfilled trough installation. Detailed cable data are given in Appendix A. The Gauss–Seidel (GS) method (2) and the successive relaxation method (3) are used to compute the temperature inside the trough and the ampacity; see Table I. While the successive relaxation method converges in five iterations when it fulfills (1) with a maximum error of 0.5°C, the iterative GS approach using (2) does not converge. In the latter case, the results for temperature inside the trough and current, toggle between two extremes. Starting from different initial temperatures anywhere between the two extremes, 34 °C and 78 °C, does not change the outcome. The successive relaxation method consistently converges in a few iterations while the GS yields divergent solutions. The successive relaxation method has been programmed in the commercial program CYMCAP [14].

III. VALIDITY RANGE OF THE IEC STANDARD METHOD

The physical problem that we solve consists in computing the maximum temperature attained by a cable (or set of cables) installed in a trough flush with the soil surface (as shown in Fig. 2).

To establish the validity range of the formula in the IEC Standard (1), we compare the results against hundreds of transient finite-elements (FEM) simulations varying the following parameters: a) trough size (perimeter); b) ambient air temperature; c)

TABLE I
CONVERGENCE PROPERTIES OF METHODS (2) AND (3)

Iteration Number	Equation (2)		Equation (3)	
	Trough Air Temperature [°C]	I (A)	Trough Air Temperature [°C]	Current
0	25	1396	25	1396
1	88.13	188	56.56	963
2	26.15	1383	55.82	977
3	86.94	250	55.85	974
4	27.02	1372	55.83	976
5	85.97	289	converged	converged
…			-	-
71	34.14	1284	-	-
72	78.4	531	-	-
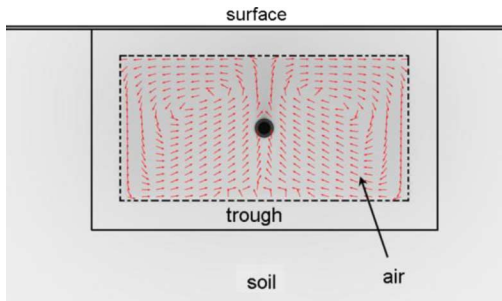
Fig. 2. Unfilled trough with lid flush with the soil surface.

cable operating temperature (total losses); d) trough aspect ratio; e) position of cables; and f) effects of solar radiation.

The physics of the heat-transfer phenomenon in an unfilled trough enables distinguishing between three study conditions (or study times). This is so because the temperature of the cable can reach three different steady-state temperatures depending on the modeling conditions. Consider the case of a single cable installed at the center of the trough in Fig. 2. Depending on where the ambient temperature can be considered unaffected by the cable, we can classify the study into three categories:

1) *Air adiabatic* is the case when the temperature at the inner surface of the trough can be considered constant. This is equivalent to the conditions of the IEC standard. This situation is only adequate for short duration transient studies (a few hours); see Fig. 3.
2) *Trough adiabatic* is when the temperature at the outer surface of the trough can be considered constant. This situation is adequate for midterm transients (under a day); see Fig. 3.
3) *Non-adiabatic* is when an infinitely deep and wide soil is considered. This situation is adequate for long-term transients and it represents the true conditions yielding to the final steady state. The attainment of the steady-state temperature may take longer than a month.

Starting from a soil ambient temperature of 20 °C, transient heat-transfer FEM simulations are performed until steady state is reached as in Fig. 3. This is necessary to properly deal with the unpredictability of local vortexes of the air convection process in the trough; visible in Fig. 2. One can see from Fig. 3 that all three curves have the same beginning, but they separate as the different physical conditions start to have influence. When the same ambient temperature is used for the three cases,
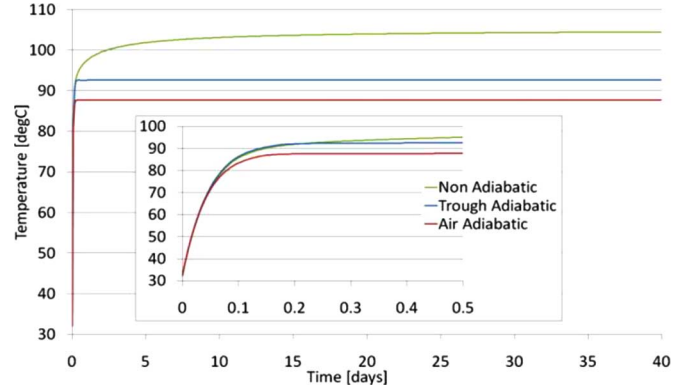
Fig. 3. Plot of temperature versus time for air adiabatic, trough adiabatic, and nonadiabatic conditions.

the nonadiabatic conditions yield the highest conductor temperature. This is because the power loss in the cable increases the temperature (although slowing and slightly) of the close surroundings.

All finite-element simulations of this paper were performed using the conjugate heat-transfer module of COMSOL Multiphysics [15], which enables the representation of problems involving conduction, convection, and radiation. Using the conjugate heat-transfer module, the set of nonlinear equations that are solved simultaneously with the finite elements method is:

the Navier–Stokes equation

$$\rho \frac{\partial u}{\partial t} + \rho(u \cdot \nabla)u = -\nabla p + \mu \nabla^2 u + \rho g \qquad (4)$$

the continuity equation

$$\frac{\partial \rho}{\partial t} + \nabla \cdot (\rho u) = 0 \qquad (5)$$

and the energy equation

$$\rho C_p \frac{\partial T}{\partial t} + \rho C_p u \cdot \nabla T = \nabla \cdot (k \nabla T) + Q \qquad (6)$$

where T is the temperature at a point, u is the air particle velocity field, ρ is the density, p is the pressure, g is the acceleration due to gravity, k is the thermal conductivity, C_p is the specific heat, and Q is the heat generated. For the air domain, COMSOL solves the complete computational fluid dynamics (CFD) problem (i.e., specific heat C_p, thermal conductivity k, density ρ, and all variables derived from them, such as viscosity ν are functions of temperature and pressure).

A time-dependent segregated solver is used for each mode of physics separately. Each model consisted of anywhere from 16 000 to more than 60 000 triangular mesh elements and 22 000 to 101 000 degrees of freedom, depending on the size of the trough and complexity of the simulation. In order to reduce the computational effort, the construction of the cable used in the simulations was kept simple (see Appendix A); however, the methods of this paper are completely general and applicable to any cable construction. Time to completion can vary from 20 h to simulate 2 days to up to 82 h for a 5-day-long simulation using a server that has 24 cores in its central processing unit (CPU) running at 3.33 GHz each as well as 96 GB of DDR3 random-access memory (RAM).

TABLE II
CALCULATED MAXIMUM TEMPERATURE OF THE CONDUCTOR

Perimeter Length [m]	Trough Dimensions		Ambient Temp. [°C]	Losses [W/m]	Non-Adiabatic Finite Elements 2 – Days	IEC Standard Calculations [°C]		Model of Reference [10]		Circuit (Fig. 8) 2 - Days	
	Width [m]	Height [m]				Temp. [°C]	% Difference to FEM	Temp. [°C]	% Difference to FEM	Temp. [°C]	% Difference to FEM
1	0.32	0.34	20	62.07	93.16	90	-3.40	87.05	-7.02	93.40	0.25
1	0.32	0.34	45	38.31	91.26	90	-1.38	88.20	-3.47	91.11	-0.16
1	0.32	0.34	32	50.45	92.15	90	-2.33	87.60	-5.19	92.11	-0.04
2	1	0.5	20	78.32	99.65	90	-9.68	88.91	-12.07	97.67	-2.03
2	1	0.5	32	63.70	99.65	90	-9.68	89.19	-11.72	96.01	-3.79
2	1	0.5	45	48.10	96.62	90	-6.85	89.44	-8.02	94.30	-2.45
3	1	1	20	79.39	100.90	90	-10.80	89.19	-13.13	97.98	-2.98
3	1	1	32	64.37	98.20	90	-8.35	89.35	-9.90	96.10	-2.18
3	1	1	45	48.35	95.31	90	-5.57	89.47	-6.52	94.15	-1.23
4	2	1	20	87.39	104.81	90	-14.13	90.34	-16.02	104.48	-0.32
4	2	1	32	70.89	101.47	90	-11.30	90.32	-12.35	101.47	0.00
4	2	1	45	53.30	97.90	90	-8.07	90.24	-8.49	98.31	0.42

A. Varying the Perimeter

According to IEC standard 60287, the perimeter of an unshaded trough that is effective for heat dissipation includes vertical walls and the floor. Varying the perimeter length, in effect, increases the trough size while providing more area for heat dissipation.

To study the effect of different perimeter lengths on the maximum temperate reached within the trough, numerous nonadiabatic transient FEM simulations are performed for a time of two days. Identical cables at ambient temperatures of 20 °C, 32°C, and 45 °C were used with varying losses calculated with IEC standard 60287 to obtain a maximum temperature of 90 °C. The results of these simulations, shown in Table II, reveal that the IEC Standard method is adequate for relatively small troughs (perimeter 1 m) for short periods of time. However, the method is less accurate for larger troughs, where the errors could be close to 15% on the optimistic side. After two days of simulation time, the cables had not yet reached the nonadiabatic condition, a longer simulation length would result in a greater maximum temperature further increasing the difference by which the IEC standard underestimates the maximum temperature. Similar results to those of the IEC standard were obtained with the model of [10]; see Table II. The table also shows the results of the model proposed in this paper (Section IV). One can see that our model matches very well with the FEM simulations.

B. Constant Internal Perimeter—Varying Aspect Ratio

In this section, we vary the trough aspect ratio by keeping the nonexposed perimeter (p) constant; see Fig. 4. Varying the aspect ratio (width/height) changes the convection pattern that may have an influence in the attained maximum temperature.

A model with a perimeter effective for heat dissipation, in the IEC sense, of 2 m is selected to give a large range of different aspect ratios. According to the standard, the walls and floor of the trough are the areas available for heat transfer. The smallest
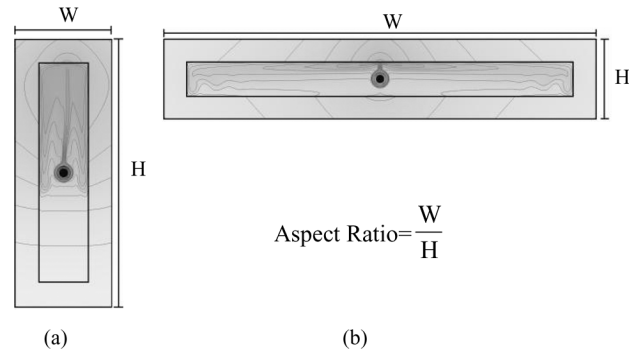
Fig. 4. Troughs flush with the soil showing the isothermals. (a) Small aspect ratio 0.22. (b) Large aspect ratio 2.25.

aspect ratio of 0.22 is obtained from a trough with a width of 0.2 m and a height of 0.9 m [Fig. 4(a)] while the largest aspect ratio of 11.33 is obtained from a trough with a width of 1.7 m and a height of 0.15 m [Fig. 4(b)]. Eighteen troughs of different aspect ratios were simulated with FEM assuming constant losses and for two different ambient temperatures of 32 °C and 45 °C. (See the results in Fig. 5.) Cables in all cases were kept at the center of the trough as if supported by brackets. It can be confirmed, as inferred in the IEC standard, that the aspect ratio does not have an important effect on the maximum temperature obtained since differences of only a few tenths of a degree can be seen. It can be noted from Fig. 4 that the different aspect ratios do produce completely different fluid flow patterns within an unfilled trough; this, however, does not seem to affect the steady-state maximum temperature.

C. Varying Position of Cables

Per IEC Standard 60287, the cable temperature (or ampacity) depends on the distance a cable is positioned from the vertical wall in air (therefore in the trough as well). In that standard, there is no account for the horizontal position of the cable in the
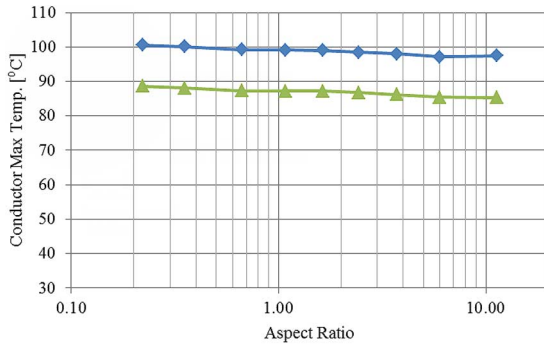
Fig. 5. Aspect ratio versus maximum conductor temperature for ambient temperatures of 45 °C and 32 °C.

Fig. 6. Horizontal and vertical cable position versus maximum conductor temperature at the steady state.

TABLE III
CALCULATED MAXIMUM TEMPERATURE OF THE CONDUCTOR

Perimeter Length [m]	Trough Dimensions		Ambient Temp. [°C]	Losses [W/m]	Temperature [°C] at Position		% Difference Center to Bottom Position
	Width [m]	Height [m]			Center	Bottom	
1	0.32	0.34	32	50.45	83.214	72.956	-14.06
2	1	0.5	32	63.70	92.664	81.861	-13.20
3	1	1	32	64.37	92.269	81.391	-13.37

trough, whether it is near the top, center, or resting on the floor. Additional information on derating factors for cables installed very close to floors or ceilings is available in IEC 60364-5-52 (withdrawn) [11] and the book by Anders [12]. Those derating factors would apply to the arrangements discussed in this section of the paper. Note, however, that those factors were derived from a limited number of tests.

A comparative study was carried out by performing FEM simulations of several concrete trough sizes with a single current carrying cable positioned at the center and bottom of the trough. When the cable is positioned sitting on the floor, a small amount is compressed into the floor to account for the compression of the insulation due to the cable's weight. It can be seen in Table III that, on average, the maximum temperature reached during steady state decreased by 13.54% when the cable was positioned sitting on the floor of the trough. It should be noted that these simulations were conducted under trough adiabatic conditions to verify the resulting temperature drop when cables are placed on the floor of the trough.

Several cases were also carried out to study the effects of cable position when not in direct contact with the floor. A single cable with constant losses was moved to different positions within a trough of constant size and ambient temperature. The horizontal position of the cable was varied from a distance considered "attached to the wall" by IEC Standard 60287-2-1 (Table 2), to the center of the trough. The vertical position of the cable was varied in a similar fashion with the results from both being presented in Fig. 6. The points on the graph represent the center of the cable; therefore, the distance of the outer surface of the cable to the wall is a radius ($r = 30.93$ mm) closer to the wall. The most significant difference of 5.32% compared to the maximum temperature obtained with the IEC standard occurred when the cable was at the closest distance to the ceiling of the trough, limiting air flow around the cable. This, however, is not a significant difference and is an unlikely situation for practical purposes. The best conditions occur when the cable is near the floor.
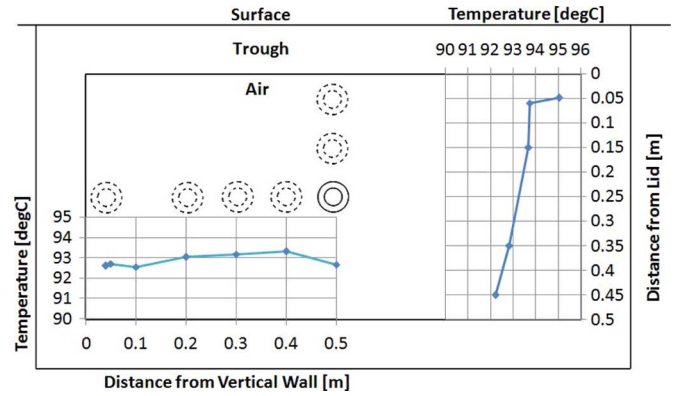
It seems that what Table 2 in IEC Standard 60287-2-1 suggests (i.e., the necessity for alternative values) for the constants Z, E and g when the outer surface of a single cable is positioned less than $0.3 \times D_e^*$, where D_e^* is the external diameter of the cable, away from the vertical wall, is not accurate. As seen by the two points closest to the wall in Fig. 6, the exterior of the cable was positioned with a clearance of $0.3 \times D_e^*$ as well as $0.146 \times D_e^*$ away from the vertical wall. The latter is close, but does not touch the wall and is considered "attached to the wall" by IEC Standard 60287-2-1. According to the standard, for the trough dimensions used in Fig. 6, the temperature difference between the two positions should be 2.46 °C. Our results show, however, that the difference in maximum temperature varies by only 1/10th of a degree, suggesting that the distance to the wall does not play an important role. Further research is necessary before drawing any definitive conclusions.

D. Varying the Intensity of Solar Radiation

According to IEC Standard 60287, in order to account for the effects that solar radiation has on the temperature within an unfilled trough, "any portion of the perimeter, which is exposed to sunlight is therefore not included in the value of p." In our case, since we assume that the trough is flush with the surface, we have excluded the lid from the calculation of p. This increases ΔT, therefore increasing the effect the trough has on the maximum free-air ambient temperature of the cable. In the ECRC report, which summarizes the measurements made by the ERA Technology, the effect of solar radiation is considered by increasing the temperature inside the trough by an additional 9 °C compared to the temperature rise due to the losses inside the trough [10]. Although this value might be suitable for Northern Europe, Canada, and the Northern U.S. similar to where the
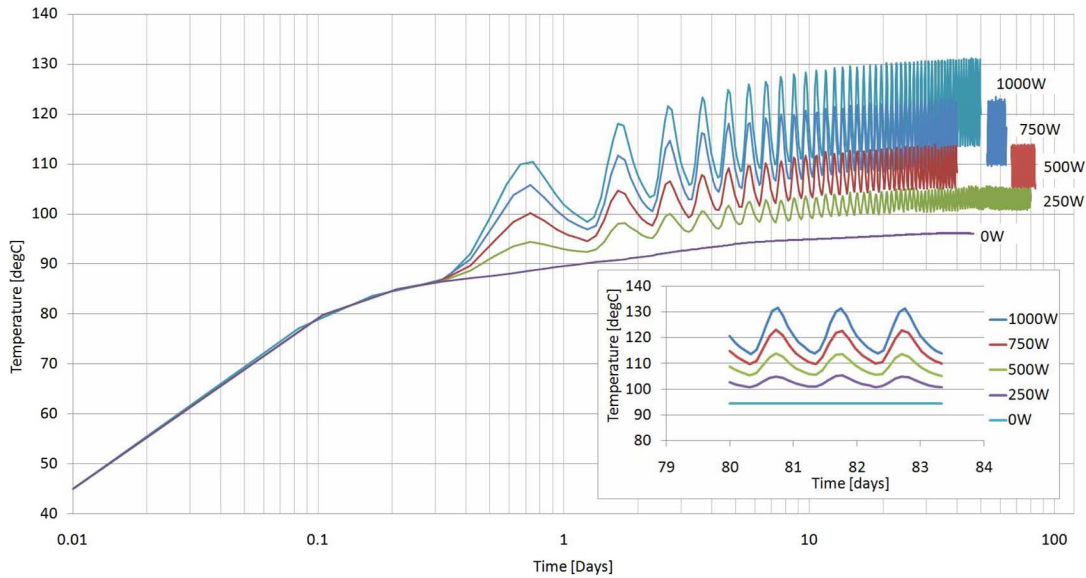
Fig. 7. Maximum temperature as a function of time showing the effects of solar radiation incident on the trough lid and surrounding soil.

measurements are made, the appropriate value depends on the intensity of solar radiation and the length of exposure.

Fig. 7 shows the temperature swing in the trough associated with the variations of the intensity of solar radiation on a daily basis. One can see that at the beginning, for about 0.3 of a day (7 h), the temperature rise is dominated by the losses in the cable and the solar radiation plays a reduced role. A detailed view of three days of temperature rise and fall can be seen in the insert in Fig. 7. In Fig. 7, the ends of the 1000-, 750-, and 500-W plots have been cut so the temperature swing can be seen in the graph. The physical characteristics of the materials used in the lid of the trough as well as the soil also play a large role in the resulting temperature swing within the trough.

Through the analysis of finite-elements results, a model has been derived in this paper to account for not only daily variations in the solar radiation, but also for soil and trough material properties. These results will be discussed in Section IV.

E. Long-Duration Transients (Nonadiabatic)

In order to illustrate the effects that the trough and surrounding soil have on the maximum temperature achieved in a cable and subsequent ratings, long duration simulations were completed for a length of 40 days. The three study conditions: air adiabatic, trough adiabatic, and nonadiabatic were used with a 3-m perimeter length trough, 32 °C ambient temperature, and losses of 63.70 W/m with a single cable at the center of the trough. The temperature rise of each simulation can be seen in Fig. 3 with a more detailed view of the first half of day 1 inset within the graph. In the air adiabatic case, steady state is reached within 4.8 h with a maximum temperature of 87.67 °C. Trough adiabatic reached 92.42 °C at steady state within 8.6 h. The nonadiabatic case reached a maximum of 104.43 °C after 40 days and was still not at true steady state, results that are expected for the most realistic of all study conditions.

F. Surface Emissivity

The surface emissivity of a material is a measure of the material's ability to emit energy via radiation. The radiated heat flux depends on emissivity, surface area, color, and chemical composition. Surface emissivity between two objects can vary greatly as distance and orientation change.

IEC standard 60287 neglects any affect due to surface emissivity of the materials used in the cable within the trough and of the trough itself. A comparative study was performed using finite elements both with and without the physics associated with the affects of surface emissivity.

All results point to surface emissivity contributing at least 10% of temperature rise. In most cases, the contribution is in the order of 20%. With these large differences as well as the prospect of vastly different materials being used, it is obvious that surface emissivity plays an important role in ampacity calculations in concrete troughs and needs to be considered in the calculation methods.

IV. THERMAL EQUIVALENT CIRCUIT

The ampacity of cables in unfilled troughs can be computed methodologically from the solution of a physically sound model. The proposed thermal model is a circuit as shown in Fig. 8; it consists of a set of series resistances, shunt capacitors, and heat sources. The circuit considers all of the elements involved in the heat-transfer problem. In particular, the following components are represented explicitly: 1) the cable (only the conductor and insulation are depicted in the figure, but the method is compatible with the models of all complex cable constructions supported by the IEC standards by substituting the appropriate circuit model in the region marked "cable" in Fig. 8); 2) the convection of air in the trough; 3) the radiation from cable to the trough, the trough thickness and material, and the soil; 4) the intensity of solar radiation; 5) the convection to the open air; and 6) the ambient temperature.
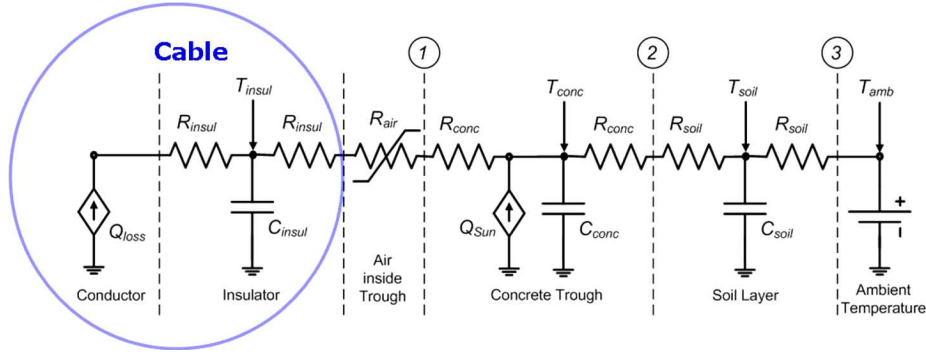
Fig. 8. Thermal circuit for cables in unfilled troughs.

The losses in the cable are calculated per [4]. The thermal resistances of the cable layers are calculated per [6]. The thermal capacitances of the cable (conductor, insulator, sheath, etc.) can be evaluated following the equations in [20]. The thermal resistance of air is nonlinear and is evaluated in Section V. R_{conc} and C_{conc} are the thermal resistance and capacitance (per unit length), respectively, of the trough and are given by

$$R_{\mathrm{conc}} = \Delta x / k A_{\mathrm{cs}}$$
$$C_{\mathrm{conc}} = C_p \rho A_{\mathrm{cross}} \tag{7}$$

where Δx is the thickness of the concrete trough, and k and A_{cs} are the conductivity and surface area of the layer. C_p, ρ and A_{cross} are the specific heat, density, and cross-sectional area of the concrete trough, respectively. The heat source Q_{sun} applied to the concrete layer represents the incident solar heat flux on the trough/soil surface. To study the thermal rating of cables protected from solar radiation, this factor is set to zero. The soil resistance and capacitance may be evaluated from [19] and [20]. An algorithm-based approach to evaluate the soil resistance and capacitance is given in [21]. The voltage at each node represents the temperature of the particular component in the circuit.

The comparison of conductor temperature between finite-element simulations and the proposed model is given in the last two columns of Table II. The results show very good matching with respect to FEM; the maximum error is less than 4%. A set of transient experiments, including the cyclic variations of the intensity of solar radiation, was performed to further validate the model. The comparison of the results between the model of Fig. 8 and the results from FEM for different intensities of solar radiation are presented in Fig. 9. The maximum error at the upper and lower peaks is 5.24%, which is very good considering the complexity of the physics involved in the analysis of heat transfer in unfilled troughs.

V. Thermal Resistance of Air

The IEC standard procedure for calculating maximum temperature utilizes the formula for cables in free air with a modified ambient temperature. The method implicitly accounts for the heat transferred by radiation. The radiative heat flux from cable to trough can account for 20%–30% of the total heat flux
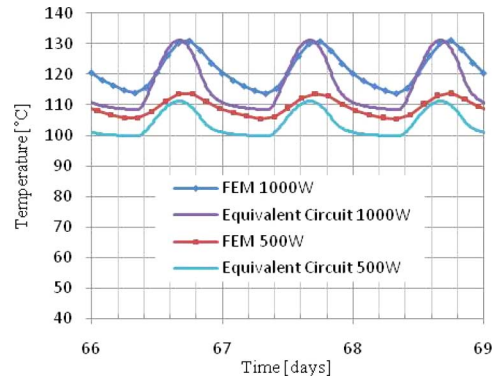
Fig. 9. Temperature swing within the trough due to solar radiation from FEM and the thermal circuit.

for operating temperatures around 90 °C and is hence important for this study.

The net heat flux exchange via radiation between the cable and the trough is given by ([15], [16], [22])

$$q_{\mathrm{rad}} = h_{\mathrm{rad}} A (T_s - T_{\mathrm{conc}}) \tag{8a}$$
$$h_{\mathrm{rad}} = \varepsilon \sigma (T_s + T_{\mathrm{conc}}) \left(T_s^2 + T_{\mathrm{conc}}^2\right) \tag{8b}$$

where h_{rad} is the radiative heat-transfer coefficient and σ is the Stefan–Boltzmann's constant; ε is the emissivity of the cable surface, with area A, dissipating radiative heat; and T_s and T_{conc} are the temperatures of the cable surface and the trough, respectively.

Equations (8a) and (b) can be written using the view factor (F_{12}) in the following way [22]:

$$q_{\mathrm{rad}(1-2)} = F_{12} \varepsilon \sigma A \left(T_1^4 - T_2^4\right) \tag{8c}$$

where $q_{\mathrm{rad}(1-2)}$ is the amount of radiated heat flux from the cable to the trough; and T_1 and T_2 are the surface temperatures of the cable and trough, respectively. F_{12} can range from zero (for two surfaces spaced very far apart) to 1 (when the cable is totally enclosed by the trough as in our case). Equations (8a) and (b) give the possibility of varying emissivity depending on the material of the outermost cable cladding, whereas the IEC standard [6] uses a fixed value. We remark that (8c) can be used

TABLE IV
CALCULATION OF THE NUSSELT NUMBER FROM THE RAYLEIGH NUMBER [16]

No.	Range Ra_D	C	m
1	$10^{-10} - 10^{-2}$	0.675	0.058
2	$10^{-2} - 10^{2}$	1.02	0.148
3	$10^{2} - 10^{4}$	0.85	0.188
4	$10^{4} - 10^{7}$	0.48	0.25
5	$10^{7} - 10^{10}$	0.125	0.333

to compute the mutual radiation effects between cables in air (or troughs) with the proper view factor.

The dominant factor of the heat transfer on the surface of the cable is convection. The convective heat-transfer coefficient h_{conv} can be computed from the Rayleigh number Ra_D [16] and [18] (defined in Appendix B) and given in Table IV.

$$\mathrm{Nu} = C \mathrm{Ra}_D^m \tag{9}$$

where Nu is the Nusselt number [16], [17].

$$h_{\mathrm{conv}} = \mathrm{Nu} k / D \tag{10}$$

where k is the thermal conductivity of air or the medium surrounding the cable with diameter D.

The equivalent thermal resistance for convection is given by

$$R_{\mathrm{conv}} = \frac{1}{h_{\mathrm{conv}} A} \tag{11}$$

and that for radiation is

$$R_{\mathrm{rad}} = \frac{1}{h_{\mathrm{rad}} A}. \tag{12}$$

Since both phenomena occur simultaneously, the total resistance is the parallel combination of (11) and (12).

VI. CONCLUSION

A numerically robust method, based on relaxation, has been proposed for the computer implementation of the IEC Standard method for rating cables installed in unfilled troughs. Using hundreds of finite-element simulations, the validity range of the standardized equations has been established. The IEC method works well for small troughs, and the error increases slightly as the trough size increases. In addition, it has been confirmed that the trough aspect ratio does not play a significant part. It has also been corroborated, as implicitly stated in the standard, except for cables lying on the floor (or too close to the ceiling), that the position of the cables is not important. It has been shown that the intensity of solar radiation and trough and soil parameters, that are ignored by the IEC standard, have an important influence. To solve this problem, a physically sound model has been proposed in this paper for the thermal rating of cables installed in unfilled troughs. The adopted model is compatible with the

IEC standard methods since it is an equivalent circuit where all parameters can be computed from the geometrical dimension and the physical forces (heat sources and sinks) acting on the installation.

APPENDIX A
CABLE DATA
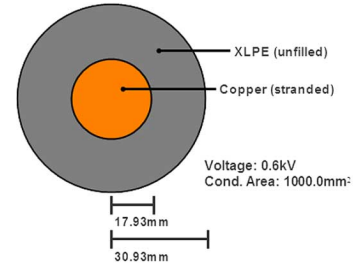
APPENDIX B
RAYLEIGH NUMBER

$$\mathrm{Ra}_D = \mathrm{Gr}_D \mathrm{Pr} \tag{13}$$

where Gr_D is the Grashoff's number and Pr is the Prandtl number.

$$\mathrm{Gr}_D = \frac{g\beta(T_s - T_\infty)D^3}{\nu^2} \tag{14}$$

$$\mathrm{Pr} = \frac{C_p \mu}{k} \tag{15}$$

where g is the acceleration due to gravity, β is the volumetric thermal expansion coefficient, v is the kinematic viscosity, C_p is the specific heat capacity at constant pressure, and μ is the dynamic viscosity.

REFERENCES

[1] G. Anders, *Rating of Electric Power Cables: Ampacity Computations for Transmission, Distribution, and Industrial Applications*. New York: IEEE, 1997.
[2] J. H. Neher and M. H. McGrath, "The calculation of the temperature rise and load capability of cable systems," *AIEE Trans., Part III—Power App. Syst.*, vol. 76, pp. 752–772, Oct. 1957.
[3] *IEEE Standard Power Cable Ampacity Tables*, IEEE Std. 835–1994, 1994.
[4] *Electric Cables—Calculation of the Current Rating—Part 1: Current Rating Equations (100% Load Factor) and Calculation of Losses—Section 1: General*, IEC Standard 60287-1-1 (1994-12), 1994.
[5] *Electric Cables—Calculation of the Current Rating—Part 1: Current Rating Equations (100% Load Factor) and Calculation of Losses—Section 2: Sheath Eddy Current Loss Factors for two Circuits in Flat Formation*, IEC Standard 60287-1-2 (1993-11), 1993.
[6] *Electric Cables—Calculation of the Current Rating—Part 2: Thermal Resistance—Section 1: Calculation of the Thermal Resistance*, IEC Standard 60287-2-1 (1994-12), 1994.
[7] *Electric Cables—Calculation of the Current Rating—Part 2: Thermal Resistance—Section 2A: A Method for Calculating Reduction Factors for Groups of Cables in Free air, Protected From Solar Radiation*, IEC Standard 60287-2-2 (1995-05).

[8] *Electric Cables—Calculation of the Current Rating—Part 3: Sections on Operating Conditions—Section 1: Reference Operating Conditions and Selection of Cable Type*, IEC Standard 60287-3-1 (1995-07), 1995.

[9] P. Slaninka, "Thermal resistance of a cable channel," *Bull. Vuki*, vol. 18, no. 5, pp. 212–221, 1965.

[10] G. Anders, "Ampacity calculations for cables in shallow troughs," *IEEE Trans. Power Del.*, vol. 25, no. 4, pp. 2064–2072, Oct. 2010.

[11] *Electrical Installations of Buildings—Selection and Erection of Electrical Equipment—Wiring Systems*, IEC 60364-5-52, 2001, 2nd ed. 2001-08 (withdrawn).

[12] G. Anders, *Rating of Electric Power Cables in Unfavorable Environments*, 1st ed. Hoboken, NJ: Wiley/IEEE, 2005.

[13] H. N. Bertram, "On the convergence of iterative solutions of the integral magnetic field equation," *IEEE Trans. Magn.*, vol. MAG-11, no. 3, pp. 928–933, May 1975.

[14] CYME International T&D Inc. St-Brunto. Quebec, 2010, CYMCAP Users' Guide version 5.04.

[15] "Comsol multiphysics," in *Heat Transfer Module User's Guide*. Burlington, MA: Comsol AB Group, 2006, pp. 1–222.

[16] O. G. Martynenko and P. P. Khramtsov, *Free Convective Heat Transfer*. Berlin, Germany: Springer-Verlag, 2005.

[17] R. B. Bird, W. E. Stewart, and E. N. Lightfoot, *Transport Phenomena*, 2nd ed. Hoboken, NJ: Wiley, 2007.

[18] S. Kakac and Y. Yener, *Convective Heat Transfer*, 2nd ed. Boca Raton, FL: CRC, 1995.

[19] *Calculation of the Cyclic and Emergency Current Rating of Cables—Part 2: Cyclic Rating of Cables Greater Than 18/30 (36) kV and Emergency Ratings of Cables for all Voltages*, IEC Standard 60853-2 (1989-07).

[20] *Calculation of the Cyclic and Emergency Current Rating of Cables—Part 1: Cyclic Rating Factor for Cables up to and Including 18/30 (36) kV*, IEC Standard 60853-1 (1985-01).

[21] M. Sakata and S. Iwamoto, "Genetic algorithm based real-time rating for short-time thermal capacity of duct installed power cables," in *Proc. Intell. Syst. Appl. to Power Syst. Int. Conf.*, 1996, pp. 85–90.

[22] J. P. Holman, *Heat Transfer*, 6th ed. New York: McGraw-Hill, 1986.

Matthew Terracciano received the B.S. degree in electrical engineering from the Polytechnic Institute, New York University, in 2010 and is currently pursuing the M.Sc. degree in electrical engineering.

His research interests include cable ampacity and thermal analysis.

Sujit Purushothaman (S'09) received the B.E. degree in electrical engineering from Mumbai University (Sardar Patel College of Engineering), Mumbai, India, in 2005. He received the M.Sc. degree in electrical engineering from the Polytechnic Institute of New York University, Brooklyn, NY, in 2009, and is currently pursuing the Ph.D. degree in electrical engineering at Polytechnic Institute, New York University, Brooklyn, NY.

His work experience includes testing and development of medium-voltage switchgear for Siemens India. His research interests include power system transients, subsynchronous resonance damping, machine design and modeling, and thermal modeling of electrical machines.

Francisco de León (S'86–M'92–SM'02) received the B.Sc. and M.Sc. (Hons.) degrees in electrical engineering from the National Polytechnic Institute, Mexico City, Mexico, in 1983 and 1986, respectively, and the Ph.D. degree in electrical engineering from the University of Toronto, Toronto, ON, Canada, in 1992.

He has held several academic positions in Mexico and has worked for the Canadian electric industry. Currently, he is an Associate Professor at the Polytechnic Institute, New York University, Brooklyn, NY.

Alireza Vashghani Farahani (M'02) received the B.Sc. degree in applied physics from Isfahan University, Isfahan, Iran, in 1990, and the M.Sc. degree in physics from Shiraz University, Shiraz, Iran, in 1995. He received the M.Sc. and Ph.D. degrees in electrical engineering from the University of Toronto, Toronto, ON, Canada, in 2003 and 2010, respectively.

Since 2007, he has been with CYME International T&D. His research interests are numerical modeling of microwave magnetic components, time-domain finite-element modeling of heat transfer, and real-time temperature rating (RTTR) applications.